Article

A Quantum Mechanical Analysis of the Electronic Response of BN Nanocluster to Formaldehyde

Vahid Vahabi[1] and Hamed Soleymanabadi[2]*

1. Department of Chemistry, College of Science, Central Tehran Branch, Islamic Azad University, Tehran, Iran
2. Young Researchers and Elite club, Shahr-e-Rey Branch, Islamic Azad University, Tehran, Iran
*Corresponding author: Tel.: +98-918-3388300; E-mail: soleymanabadi.h@gmail.com

Abstract. It has been previously demonstrated that the electronic properties of pristine BN nanotubes and graphene-like sheets are not sensitive toward presence of H_2CO gas. Here, the adsorption of H_2CO on the external surface of $B_{12}N_{12}$ nano-cage is studied using X3LYP and Minnesota density functional calculations. Three different adsorption behaviors were found including physisorption, chemisorption, and chemical functionalization. Gibbs free energy changes at room temperature and 1 atm pressure is in the range of -0.07 to -2.00 eV (X3LYP). The HOMO-LUMO energy gap of the cluster dramatically decreases after the H_2CO chemisorption. Thus, $B_{12}N_{12}$ nanocluster may be used in gas sensor devices for H_2CO detection.
Keywords: Nanostructures; Surfaces; Ab initio calculations; Electronic structure.

Resumen. Se ha demostrado previamente que las propiedades electrónicas de nanotubos y sábanas tipo grafeno BN prístinos no son sensibles a la presencia de H_2CO gaseoso. Aquí se estudia la adsorción de H_2CO sobre la superficie externa de nano-cajas $B_{12}N_{12}$ utilizando cálculo de funcionales de la densidad X3LYP y desarrollados en Minnesota. Se encontraron tres comportamientos de adsorción diferentes incluyendo fisisorción, quimisorción y funcionalización química. Los cambios de energía libre de Gibbs, a temperatura ambiente y presión de 1 atm, se encuentran en el rango de -0.07 a -2.00 eV (X3LYP). La brecha de energía HOMO-LUMO del cúmulo disminuye dramáticamente después de la quimisorción de H_2CO. Por lo tanto, los nano-cúmulos $B_{12}N_{12}$ podrían usarse en dispositivos sensores de gases para la detección de H_2CO.
Palabras clave: Nanoestructuras; Superficies; cálculos ab-initio; Estructura electrónica.

1. Introduction

Formaldehyde (H_2CO) is an important reactive intermediate product in tropospheric hydrocarbon oxidation initiated by the OH radical. Its concentration in the atmosphere is in the range of 1 to 10 ppb [1]. The importance of H_2CO molecule originates from its widely use in many industrial manufacturing processes due to the high chemical reactivity and good thermal stability. On the other hand, it is a well-known pollutant that is emitted through incomplete combustion processes [2]. To date, several methods have been developed to detect the H_2CO concentrations which have been reviewed comprehensively by Vairavamurthy *et al.* [3-7]. Since the discovery of fullerenes, numerous studies have been focused on the nanotubes, nanoclusters, nanocones, nanocapsules, nanoribbons, etc [8-16]. BN nanostructures are wide band gap materials, expecting to show special electronic, optical and magnetic properties such as Coulomb blockade and supermagnetism [17]. The properties of BN fullerenes are different with those of carbon fullerenes, from the viewpoint of electronic properties and thermal resistance. Geometries and stability of $(BN)_n$ (n = 4-30) nano-cages have been previously studied by various research groups [18-20]. $B_{12}N_{12}$ cluster was theoretically shown to be more stable with the structure based on decoration of truncated octahedrons in which all B vertices remain equivalent, as well as all N, and was successfully synthesized [18].

Recently, Wu *et al.* have investigated hydrogenation of a $B_{12}N_{12}$ molecule by calculations using ab initio molecular orbital theory [21]. We have previously shown [22] that $B_{12}N_{12}$ is the most stable nanocluster among different $X_{12}Y_{12}$ (X = Al or B and Y = N or P) cages. Nanostructured materials have been invoked more attention as chemical sensors due to high surface to volume ratio and high electronic sensitivity [23-29]. It has been previously demonstrated that the electronic properties of pristine BN nanotubes and graphene-like sheets are not sensitive toward presence of H_2CO gas, and cannot be used as chemical sensors [29, 30]. Here, the interaction between an H_2CO molecule and a $B_{12}N_{12}$ nanocluster is investigated using density functional theory (DFT) calculations to answer this question that whether there is a potential possibility of BN nanoclusters serving as chemical sensor to H_2CO.

2. Computational methods

Geometry optimizations, natural bond orbitals (NBO), and density of states (DOS) analyses were performed on a $B_{12}N_{12}$ nanocluster and different $H_2CO/B_{12}N_{12}$ complexes at the spin unrestricted X3LYP level [31] of theory with 6-31G (d) basis set [32] as implemented in GAMESS suite of program [33]. GaussSum program [34] was used to obtain DOS results.

Vibrational frequency calculations were performed using numerical second derivatives, verifying that all the structures are true minima with positive Hessian eigenvalues. The Gibbs free energy change (ΔG) of H_2CO adsorption at room temperature and 1 atm pressure is defined as follows:

$$\Delta G = G(H_2CO/ B_{12}N_{12}) - G(B_{12}N_{12}) - G(H_2CO) \qquad (1)$$

where $G(H_2CO/B_{12}N_{12})$ is the Gibbs free energy of complex, and $G(B_{12}N_{12})$ and $G(H_2CO)$ are the Gibbs free energies of the pristine $B_{12}N_{12}$ and H_2CO molecule, respectively. Zero-point and basis set superposition error (BSSE) corrections were included in the ΔG calculations. HOMO-LUMO energy gap (E_g) is defined as

$$E_g = E_{LUMO} - E_{HOMO} \qquad (2)$$

where E_{LUMO} and E_{HOMO} are energies of HOMO and LUMO. When we evaluate the properties of the sensor, the shift of the E_g is obtained by:

$$\Delta E_g = [(E_{g2} - E_{g1})/E_{g1}] * 100 \% \qquad (3)$$

where E_{g1} and E_{g2} are, the value of the E_g for clean $B_{12}N_{12}$ and the formaldehyde adsorbed state, respectively.

3. Results and discussion

The $B_{12}N_{12}$ (Fig. 1) nanocluster is made of six squares and eight hexagons. There are two types of individual B–N bond among the all 36 B–N bonds; one is shared by two six-membered rings (B_{66}), and another by a four- and a six-membered ring (B_{64}). The B_{64} bond (average length = 1.48 Å) is somewhat longer than the B_{66} one (average length = 1.43 Å). NBO population analysis shows a net charge transfer of 0.45 electrons from B to N atom in the surface of the cluster, indicating partly ionic nature of these bonds. Several distinct starting structures were considered for H_2CO adsorption on the cluster. For example, the oxygen or a hydrogen atom of H_2CO molecule was placed atop a hexagon or a square ring, or the molecule was located close to B_{64} or B_{66} bond so that its O and C or H atoms were close to the B and N atoms of these bonds. However, after careful relax optimization of initial structures four different
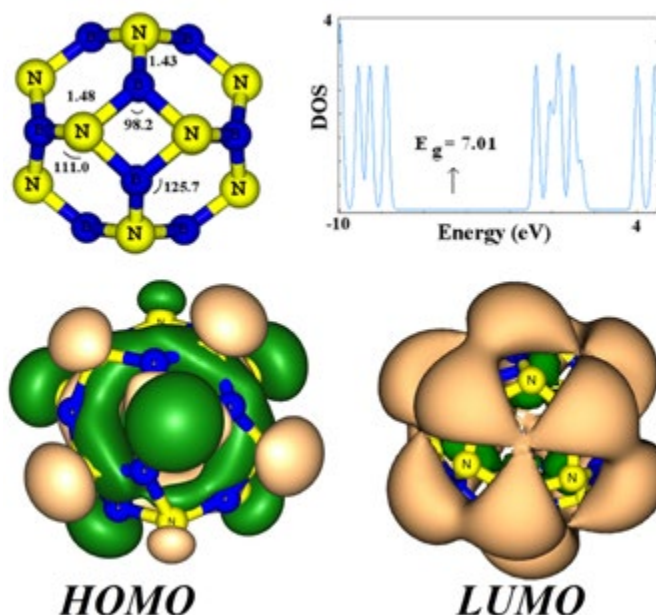

Fig. 1. Structural model, HOMO, LUMO profiles and the electronic density of states (DOS) of the $B_{12}N_{12}$ cluster. (Bonds are in angstrom and angles are in degree).

stable structures (local minima) were obtained which are shown in Figs. 2-4.

The interactions can be divided into three types: (I) Physisorption, in which H_2CO molecule weakly interacts with the cluster through van der Waals forces and less negative ΔG values (configurations **A**, Fig. 2). (II) Chemisorption, in which the ΔG value is rather more negative than that of the physisorption, and an insignificant change occurs in the geometrical parameters (configuration **B**, Fig. 3). (III) Chemical functionalization, including very strong interaction that largely deforms the structure of the cluster with bond cleavages and formations (configurations **C** and **D**, Fig. 4). The ΔG values, charge transfer, and electronic properties for the all configurations are summarized in Table 1. For the physisorption configuration **A**, the calculated values of ΔG is about -0.07 eV. Also, the corresponding interaction distances between the N atom of $B_{12}N_{12}$ cluster and the H atom of H_2CO molecule is 3.30 Å. The less negative ΔG values and large interaction distances indicate that the H_2CO molecule undergoes a weak physical adsorption due to van der

Table 1. Calculated Gibss free energy change (ΔG), HOMO energies (E_{HOMO}), LUMO energies, HOMO-LUMO energy gap (E_g), and Fermi level energy (E_F) of formaldehyde adsorbed on the $B_{12}N_{12}$. Energies are in eV. See Figs. 2, 3 and 4.

system	ΔG	LUMO	E_F	HOMO	E_g	ΔE_g (%)	[a]Q_T (|e|)
cage	-	-1.63	-5.14	-8.64	7.01	-	-
A	-0.07	-1.65	-4.77	-7.88	6.23	11	0.02
B	-0.59	-2.77	-4.59	-6.4	3.63	48	0.21
C	-2.00	-1.07	-4.23	-7.39	6.32	10	-0.04
D	-1.55	-1.09	-4.48	-7.86	6.77	3	-0.02

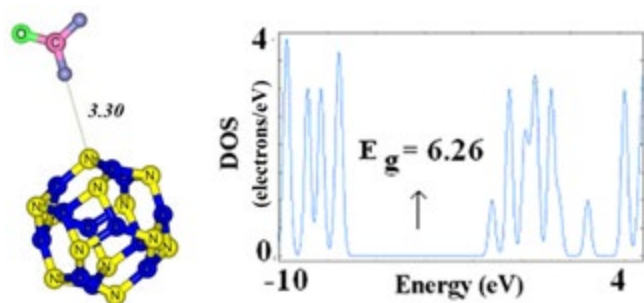[a] Q_T is defined as the total NBO charge on the formaldehyde

Fig. 2. The optimized structures of H_2CO physisorption on the $B_{12}N_{12}$ cluster and their DOSs.

Waals forces. The DOS for this configuration is shown in Fig. 2. It can be found that the DOS of pristine BN cluster (Fig. 1) is slightly affected by the adsorption of H_2CO molecule near the Fermi level and ΔE_g is negligible. The charge transfer from the H_2CO molecule to the cluster is very small (about 0.02 e).

As shown in Fig. 3, the distances between the H and O atoms of H_2CO, and the N and B atoms of the cluster in the configuration **B** are about 1.66 and 2.33 Å, respectively. The ΔG value is about -0.59 eV with a charge transfer of 0.21 e from the H_2CO molecule to the cluster. The adsorption induces a slight structural deformation to both the adsorbed molecule and the $B_{12}N_{12}$ nanocluster (Fig. 3). Angles of H-C-H and H-C-O of H_2CO are changed from 115.2° and 122.3° in their free state to 121.5° and 119.9° in the adsorbed form, and the H_2CO-adsorbed B-N bond is pulled outward from the cluster surface with the bond length increasing from 1.43 Å (pristine cluster) to

1.50 Å. In order to explore the sensitivity of $B_{12}N_{12}$ toward H_2CO molecule, we plotted the DOS of this structure and compared it with that of free cluster.

As shown in Fig. 3, the DOSs of the configuration **B** near the conduction level has an appreciate change compared to that of the pristine cluster, so that a local energy level appears after the adsorption of H_2CO molecule. Our frontier molecular analysis shows that in consistent with the energy change the LUMO shifts on the H_2CO molecule while the HOMO is still remained on the cluster (Fig. 3). Fig. 1 indicates that in the pristine cluster the HOMO and LUMO is mainly located on the N and B atoms of the cluster, respectively. However, based on the DOS analysis, the E_g value of the cluster decreases from 7.01 to 3.63 eV (48% change) upon the H_2CO molecule chemisorption on the BN cluster, which would result in the electrical conductivity change of the cluster. This phenomenon can be interpreted by the following relation [35]:

$$\sigma = A\,T^{3/2}\exp(-E_g/2kT) \tag{4}$$

Where σ is the electrical conductivity, A (electrons/$m^3K^{3/2}$) is a constant, and k is the Boltzmann's constant. According to the equation, smaller E_g at a given temperature leads to the larger electrical conductivity. It has been previously [36] shown this equation is compatible with the experimental results, and larger E_g at a given temperature leads to smaller electrical conductivity.

However, it seems that the cluster can transform the presence of the H_2CO directly into an electrical signal, suggesting
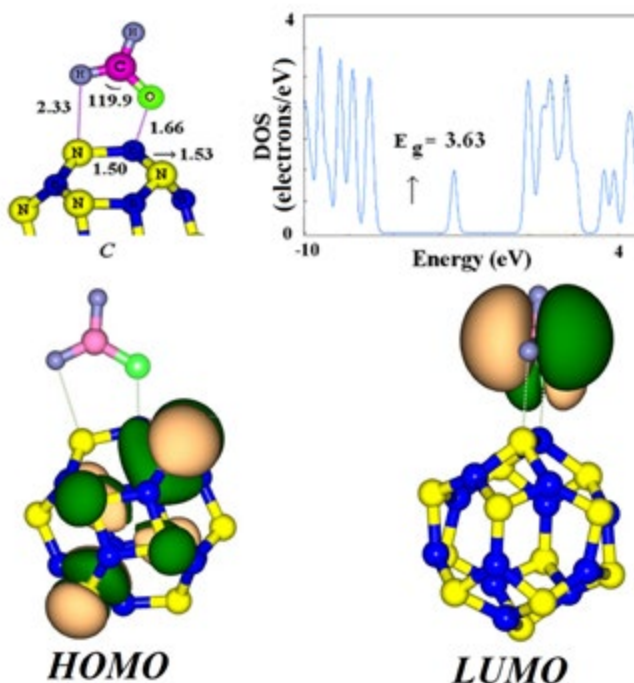

Fig. 3. The optimized structure of H_2CO chemisorption on the $B_{12}N_{12}$ cluster and its DOS plot, HOMO, and LUMO profiles.
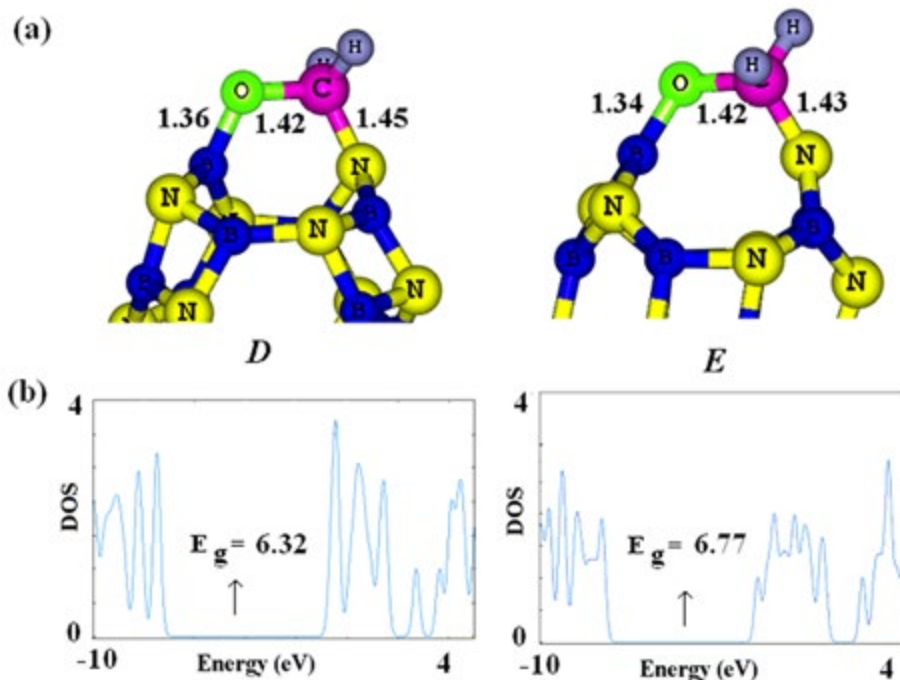
Fig. 4. The optimized structures of chemically functionalized $B_{12}N_{12}$ cluster with H_2CO and their DOSs.

that, $B_{12}N_{12}$ nanocluster may be a sensitive gas sensor toward the toxic H_2CO molecules. We found that this behavior of the BN nanocluster is in contrast to that of the BNNTs reporting by Zhang *et al.* [30]. They have theoretically investigated the adsorption of H_2CO molecule on the BNNTs, showing that the electronic properties of pristine types of these nanotubes are not affected by the adsorption of H_2CO molecule. Recovery of the sensor devices is of great importance. Based on the conventional transition state theory, the recovery time, τ, can be expressed as [36]:

$$\tau = \nu_0^{-1} \exp(-\Delta G/kT)$$

where T is temperature, k is the Boltzmann's constant, and ν_0 is the attempt frequency. According to this equation, an increase in the ΔG, will prolong the recovery time in an exponential manner.

As shown in Table 1, the ΔG of H_2CO chemisorption is about -0.59 eV which is not too large to prolong the desorption process. Finally, we considered two possible configurations that in which the cluster undergoes a strong chemical functionalization with the H_2CO molecule. To this end, the C-O bond of H_2CO molecule was horizontally located close to a B-N bond of the cluster, and then a full relax optimization was performed. The functionalized structures are shown in Fig. 4, in which the H_2CO molecule strongly adsorbed on the B_{64} (configuration **C**) or B_{66} (configuration **D**) bonds. Based on the NBO results and geometry analysis, both the B_{64} and B_{66} bonds are broken after the adsorption process and two new bonds are formed, namely, C-N and O-B. The configurations **C** and **D** have ΔG of -2.00

and -1.55 eV, with rather a small charge transfer about 0.04 and 0.02 e from the cluster to the H_2CO molecule, respectively. Geometric parameters such as the increased C-O bond length of H_2CO molecule (1.42 Å in configurations **C** and **D** compared to 1.20 Å in the isolated H_2CO), reduced H-C-H bond angle (109° as compared to 115.2° in the isolated H_2CO), and deviation of the hydrogen atoms from the original molecular plane, clearly indicate increasing p character of molecular orbitals on the C and O atoms. The NBO analysis shows that the hybridization of C and O atoms of free formaldehyde is about $sp^{2.11}$ and $sp^{1.42}$ which change to $sp^{3.14}$ and $sp^{2.85}$ in **D** configuration, respectively.

As it is shown in Table 1, the released energy during the chemical functionalization of the B_{64} bond is somewhat larger than that of the B_{66} bond. It can be interpreted by the fact that the B_{64} bond is shared by six- and four-membered rings while the B_{66} by two six-membered ones. Since a four-membered ring is thermodynamically more unstable than a six-membered one due to high strain, its cleavage is energetically easy in comparison to that of the six-membered ring, therefore, chemical functionalization of the B_{64} bond is thermodynamically more favorable than that of the B_{66} one.

The electronic properties of the cluster are not significantly changed upon the formaldehyde adsorption via these configurations. The DOS plots are shown in Fig. 4, indicating that the E_g value of cluster is slightly decreased by 0.69 and 0.24 eV in the **C** and **D** configurations, respectively. Despite the thermodynamic feasibility of the chemical functionalization, the process does not occur in room temperature due to obvious activation barriers for structure deformations. Our transition state calculations indicate that the Gibbs free energy barrier is

Table 2. Calculated HOMO, LUMO, and HOMO-LUMO energy gap (E_g) for $B_{12}N_{12}$ and complex of formaldehyde chemisorption as shown in Fig. 2 by Minnesota functionals (Energies in eV).

Functional	system	LUMO	HOMO	E_g	ΔE_g (%)
M06-L	$B_{12}N_{12}$	-1.25	-6.21	5.82	65.41
	Complex	-4.20	-8.18	2.01	
M06	$B_{12}N_{12}$	-0.71	-7.38	7.46	44.12
	Complex	-3.21	-9.28	4.17	
M06-2X	$B_{12}N_{12}$	0.17	-8.48	9.45	32.08
	Complex	-2.06	-11.24	6.41	
M06-HF	$B_{12}N_{12}$	1.21	-10.43	12.46	17.76
	Complex	-0.19	-6.21	10.24	

about 2.5 eV for these configurations. The chemical functionalization is not also an appropriate process for gas detection due to poor recovery of the sensor device which is subjected to a strong chemical functionalization. In spite of the all above-mentioned points, we think that the $B_{12}N_{12}$ can detect the H_2CO gaseous molecules through its chemisorption on the exterior surface of the cluster as discussed on here earlier (the configuration **B**).

It is well known that there is not any universal exchange-correlation functional for all purposes. One of the problems of the functionals is the calculation of HOMO, LUMO and E_g. However, our main quantity is the changes of E_g and not its absolute value. Here, we studied the effect of functionals on the electronic property results. To this aim, we repeated the calculations for the complex **B** (Fig. 2) with four Minnesota functionals M06-L [37], M06 [38], M06-2X [38], and M06-HF [39] with 0, 27, 54, and 100% Hartree Fock (HF) exchange, respectively. As shown in Table 2, the energy of HOMO, LUMO and E_g is strongly depends on the kind of functional but all functionals show significant change of E_g upon adsorption of formaldehyde which is responsible to the detection process. By increasing the percentage of HF exchange the LUMO and HOMO shift up and down, respectively, thereby increasing the E_g. Also, we have investigated the effect of basis set on the results of ΔG by repeating the calculations for the complex **B** at X3LYP level with basis sets 6-31+G(d), 6-31++G(d, p), and 6-311++G(d, p). The corresponding calculated ΔG values (Zero point and BSSE corrected) are about -0.54, -0.53, and -0.51 eV, respectively, indicating that enlarging the basis set slightly affects the results.

It should be noted that there is a difference between E_g and band gap. Band gap is defined as the energy difference between the top of the valence band and the bottom of the conduction band in the solid state, but the E_g is defined in molecular level. Matxain *et al.* [40] have shown that when $B_{12}N_{12}$ monomers form a solid structure with periodic arrangement, the band gap is somewhat smaller than the E_g of an isolated cluster. Using the generalized gradient approximation (GGA), within the Perdew-Burke-Ernzerhof (PBE) functional, they predicted that the E_g of an isolated $B_{12}N_{12}$ cluster is about 6.78 eV, while the band gap of the solid state is about 5.20 eV. This indicates that although the band gap of solid state is somewhat smaller than the E_g of the isolated $B_{12}N_{12}$ monomer, it is still large indicating semiconducting character of the solid structure.

4. Conclusion

We have studied the H_2CO adsorption on the exterior surface of $B_{12}N_{12}$ nanoclusuter, using DFT calculations. It was found that the formaldehyde can be adsorbed on the cluster surface through three different ways including physisorption, chemisorption, and chemical functionalization, with ΔG in the range of -0.07 to -2.00 eV. We showed that the electrical conductivity of the cluster is dramatically changed upon the adsorption of H_2CO molecule. Therefore, it is inferred that the $B_{12}N_{12}$ nanocluster may be a potential gas sensor for detection of H_2CO molecule.

References

1. Mine, Y.; Melander, N.; Richter, D.; Lancaster, D.G.; Petrov, K.P.; Tittel, F.K. *Appl. Phys. B*. **1997**, *65*, 771-774.
2. Dingle, P.; Franklin,P. *Ind. Built. Environ*. **2002**, *11*, 111-116.
3. Vairavamurthy, A.; Roberts, J.M.; Newman, L. *Atmos. Environ.* **1992**, *26*, 1965-1993.
4. Beheshtian, J.; Peyghan, A.; Bagheri, Z. *Struct. Chem*. **2013**, *24*, 1331-1337
5. Beheshtian, J.; Peyghan, A.; Noei, M. *Sens. Actuators B: Chem.* **2013**, *181*, 829–834
6. Noei, M.; Peyghan, A. *J. Mol. Model*. **2013**, *19*, 3843-3850
7. Rastegar, S.; Peyghan, A.; Soleymanabadi, H. *Physica E*. **2015**, *68*, 22-27
8. Peyghan, A.; Noei, M. *J. Mex. Chem. Soc.* **2014**, *58*, 46-51.
9. Nagarajan, V.; Chandiramouli, R.; Sriram, S.; Gopinath, P. *J. Nanostruct Chem*. **2014,** 4, 1-16.
10. Beheshtian, J.; Peyghan, A.; Bagheri, Z.; Kamfiroozi, M. *Struct. Chem*. **2012**, *23*, 1567-1572.

11. Nazari, M.; Ghasemi, N.; Maddah, H.; Motlagh, M. *J Nanostruct Chem*, **2014**, 4, 1-5.

12. Peyghan, A.; Soleymanabadi, H.; Bagheri, Z. *J. Mex. Chem. Soc.* **2015**, *59*, 66-72.

13. Noei, M.; Ebrahimikia, M.; Saghapour, Y.; Khodaverdi, M.; Salari, A.; Ahmadaghaei, N. *J. Nanostruct Chem.* **2015**, *5*, 213-217.

14. Talwatkar, S.; Sunatkari, A.; Tamgadge, Y.; Pahurkar, V.; Muley, G. *J Nanostruct Chem.* **2015**, *5,* 205-212.

15. Beheshtian, J.; Peyghan, A.; Bagheri, Z. J. Mol. Mod., 2013, 19, 2197-2203.

16. Beheshtian, J.; Peyghan, A.; Bagheri, Z. *Struct. Chem.* **2013**, *24*, 165-170.

17. Chopra, N.; Luyken, R.; Cherrey, K.; Crespi, V. Cohen, M. Louie, S. Zettl, A. *Science*. **1995**, *269*, 966-967.

18. Oku, T.; Kuno, M.; Kitahara, H.; Narita, I. *Int. J. Inorg. Mater.* **2001**, *3*, 597-612.

19. Seifert, G.; Fowler, P.; Mitchell, D.; Porezag, D.; Frauenheim, T. *Chem. Phys. Lett.* **1997**, *268*, 352-358.

20. Oku, T.; Narita, I.; Nishiwaki, A.; Koi, N. *Defec. Diff. Forum*. **2004**, *226*, 113-141.

21. Jia, J.; Wang, H.; Pei, X.; Wu, H. *Appl. Surf. Sci.* **2007**, *253* 4485-4489.

22. Beheshtian, J.; Bagheri, Z.; Kamfiroozi, M.; Ahmadi, A. *J. Mol. Model.*, **2012,** *18*, 2653-2658.

23. Saha, M.; Das, S. *J Nanostruct Chem*, **2014**, 4, 1-9.

24. Goodarzi, Z.; Maghrebi, M.; Zavareh, A.; Mokhtari-Hosseini, B.; Ebrahimi-hoseinzadeh, B.; Zarmi, A.; Barshan-tashnizi, M. *J Nanostruct Chem*, **2015,** *5,* 237-242.

25. Mahdavian, L. *J Nanostruct Chem*. **2012**, *3*, 1-9.

26. Saha, M.; Das, S. *J Nanostruct Chem.* **2014***, 4,* 1-9.

27. Li, L.; Feng, D.; Fang, X.; Han, X.; Zhang, Y. *J Nanostruct Chem.* **2014,** *4*, 1-8.

28. Peyghan, A.; Noei, M.; Yourdkhani, S. *Superlattices Microstruct.* **2013**, *59*, 115–122.

29. Tabtimsai, C.; Ruangpornvisuti, V.; Wanno, B. *Physica E.* **2013**, *49*, 61-67.

30. Wang, R.; Zhu, R.; Zhang, D. *Chem. Phys. Lett.* **2008**, *467*, 131-135.

31. Xu, X.; Goddard, W. *PNAS*. **2004**, *101*, 2673-2677.

32. Rassolov, V.; Ratner, M.; Pople, J.; Redfern, P.; Curtiss, L. *J. Comput. Chem.* **2001**, *22*, 976-984.

33. Schmidt, M. et al. *J. Comput. Chem.* 1993, *14*, 1347-1363

34. O'boyle, N.; Tenderholt, A.; Langner, K. *J. Comput. Chem.* **2008**, *29*, 839-845.

35. Ahmadi, A.; Hadipour, N.; Kamfiroozi, M.; Bagheri, Z. *Sens. Actuators B: Chem.*, **2012**, *161*, 1025-1029.

36. Hadipour, N.; Peyghan, A.; Soleymanabadi, H. *J. Phys. Chem. C*. 2015, *119*, 6398-6404.

37. Zhao, Y.; Truhlar, D. *J. Chem. Phys*. **2006**, *125*, 194101-194118.

38. Zhao, Y.; Truhlar, D. *Theor Chem Account*. **2006**, *120*: 215-241.

39. Zhao, Y.; Truhlar, D. *J. Phys. Chem. A*. **2006**, *110*, 13126-13130.

40. Matxain, J.; Eriksson, L.; Mercero, J.; Lopez, X.; Piris, M.; Ugalde, J.; Poater, J.; Matito, E.; Solá, M. *J. Phys. Chem. C*. **2007**, *111*, 13354-13360.